J. Hydrol. Hydromech., 71, 2023, 3, 259–270
https://doi.org/10.2478/johh-2023-0019

sciendo Journal of Hydrology and Hydromechanics Institute of Hydrology SAS

Output updating of a physically based model for gauged and ungauged sites of the Upper Thames River watershed

Ponselvi Jeevaragagam[1*], Slobodan P. Simonovic[2]

[1] Department of Water and Environmental Engineering, Faculty of Civil Engineering, Universiti Teknologi Malaysia (UTM), 81310 Johor Bahru, Johor, Malaysia.
[2] Department of Civil and Environmental Engineering, University of Western Ontario, Spencer Engineering Building, London, Ontario N6A 5B9, Canada.
[*] Corresponding author. Tel.: +6019-7604923. E-mail: ponselvi@utm.my

Abstract: This study introduces a new ANN updating procedure of streamflow prediction for a physically based HEC-HMS hydrological model of the Upper Thames River watershed (Ontario, Canada). Besides streamflow and precipitation, the updating procedure uses other meteorological variables as inputs, which are not applied in calibration of the HEC-HMS model. All the results of performance measures on training, validation and test datasets for river gauges at Mitchell and Stratford revealed that the ANN updated models have performed better than the HEC-HMS model. The ANN model results were in excellent agreement with observed streamflow. The uncertainties can be associated with different input variables and different length of datasets used in the HEC-HMS model and the ANN model. The performance results suggest improvement in the *RMSE* values of the trained networks when additional meteorological data was used. The updated errors from the gauged sites of Mitchell and Stratford were used to update the streamflow values at the ungauged site of JR750 of the HEC-HMS model. While the underlying physical process in the ANN model consisting of interconnected neurons to map input-output relationships is not easily understood (in a form of mathematical equation), the HEC-HMS hydrological model can reveal useful information about the parameters of a hydrological process.

Keywords: Neural network; Bayesian; Hydrometeorology; Hydrological model; HEC-HMS.

INTRODUCTION

In any study of accurate streamflow prediction in a watershed, the integration of hydrometeorological observations and a hydrological model is essential for water resources projects and water management in river basins. Streamflow prediction is required to determine the water quantity in a watershed, so engineer can make reliable decisions on municipal water supply planning, irrigation management, industry allocations, hydropower production, design of hydraulic structures such as culverts, dams, spillways, bridges, etc., recreational opportunities, aquatic habitat protection and wildlife conservation. The rainfall-runoff model may use some hydrometeorological data in the calibration of hydrological processes to predict the streamflow hydrographs. Rainfall-runoff modeling can be done using either an empirical, physical, or physically based models. The hydrological models based on the spatial distribution of hydrological parameters can be categorized into lumped, semi-distributed or distributed (Beven, 2001; Cunderlik, 2003).

Most of the flood damage prone sites are likely located in the ungauged basins with inadequate or unavailable flow data. Various approaches are available to estimate the streamflow value at an ungauged site (Asquith and Slade, 1997; Devulapalli, 1995; Gan et al., 1991; Jennings et al., 1994; Wurbs and Sisson, 1999; Yu et al., 1997). They usually include development of the rainfall-runoff relationships using historical time-series datasets; running computer simulations with rainfall-runoff models; use of regression-based equations; and use of regionalization methods to establish the relationship between the streamflow (such as daily streamflow, monthly flow, flood volume or peak flood flows) and the various parameters of the river basin (such as mean annual precipitation, percent of impervious surface area, drainage area, mean basin elevation, mean basin slope, channel slope etc.).

Hydrological processes are represented in the deterministic physically based models by means of certain state variables and parameters described with mathematical representations of the real phenomena (Gosain et al., 2009; Refsgaard, 1996). Usually, hydrological models do not require many hydrometeorological observations for model calibration, but the evaluation of many parameters representing the physical characteristics of catchment is required (Abbott et al., 1986). The output prediction error(s) from gauged location(s) of a physically based model can also affect output error(s) at ungauged location(s). The uncertainty in a hydrological model can stem from multiple sources such as imprecise measurements, inputs and model structure (Vrugt et al., 2005). The output prediction error from a deterministic physically based model can be reduced by integrating an updating procedure by using the artificial neural network (ANN) approach. A neural network is a form of machine learning system, which uses many layers of nodes to derive high-level functions through learning the relationships between inputs and outputs without analyzing the internal structure of the hydrological processes.

Several studies reviewing the theory and applications of ANN in hydrology have been conducted (ASCE Task Committee on Artificial Neural Networks in Hydrology, 2000; Govindaraju and Rao, 2000). ANNs are useful tools to learn and model nonlinear and complex relationships of rainfall-runoff processes (Ahmad and Simonovic, 2005; Rajurkar et al., 2004), streamflow prediction (Anctil et al., 2004; Moradkhani et al., 2004) and river stage forecasting (Bhattacharya and Solomatine, 2000; Thirumalaiah and Deo, 1998). Meteorological data such as air temperature, snowmelt, air relative humidity, soil moisture,

evapotranspiration, wind direction, etc., are used in the improvement of the ANN prediction (Anctil and Rat, 2005; Aytek et al., 2008; Jain and Srinivasulu, 2006; Poff et al., 1996; Wardah et al., 2008).

Different updating schemes of neural networks are applied to predict more accurate streamflow in the study of rainfall-runoff processes at gauged watersheds (Abebe and Price, 2004; Abrahart and See, 2007; Anctil et al., 2003; Goswami et al., 2005; Xiong and O'Connor, 2002; Xiong et al., 2004). Various input-output combinations of observations and/or simulated results are successfully applied in those procedures, which reduce the associated uncertainty and improve the efficiency of the hydrological model and/or real-time streamflow forecasting. The updating approaches include the use of optimization and backpropagation methods in the ANN weight updates; use of output error of a physically based model in the streamflow forecasting; emulation of hydrological knowledge in a numerical model; and the development of a hybrid system coupled by two (or more) linear and/or nonlinear models.

This research aims to introduce a new hybrid approach integrating the physically based HEC-HMS hydrological model and the ANN model for updating streamflow values at the river gauged and ungauged site(s) of a watershed. Several additional hydrometeorological data that are not used in the calibration of the HEC-HMS hydrological model are used in the ANN training for the best accurate prediction.

MATERIAL AND METHODS

The methodology of hydrological model improvement

The general procedure of output updating of the physically based model is shown in Fig. 1. First, the physically based model is run by using input variables to compute the flow values. Next, the neural network model is applied by using available hydrometeorological observation data to improve the output error of the physically based model for the selected gauged streamflow sites in a watershed. The improved flow errors at the gauged sites are finally used to update the computed flow values of the physically based model for the corresponding ungauged sites. The steps in the proposed methodology based on the computational engine of the HEC-HMS (USACE, 2000) are summarized as follows:

1. Estimate the flow error at the gauged site of the HEC-HMS model, $e_{gHMS}(t)$

$$e_{gHMS}(t) = Q_o(t) - Q_{gHMS}(t) \tag{1}$$

2. Estimate the updated flow error(s) at the gauged site(s), $ie_{gHMS}(t)$ with ANN technique.

$$ie_{gHMS}(t) = iQ_{gHMS}(t) - Q_{gHMS}(t) \tag{2}$$

$$iQ_{gHMS}(t) = Q_{gANN}(t) \tag{3}$$

$$Q_{gANN}(t) = \text{f}(e_{gHMS}(t-1); Q_o(t-1); \text{and meteorological data}) \tag{4}$$

The flow simulated by the ANN model, $Q_{gANN}(t)$ becomes the updated flow at the gauged site, $iQ_{gHMS}(t)$. The previous and/or recent flow error, observed flow, precipitation (rainfall and snowmelt) and additional meteorological variables are used in the ANN model.

3. The updated streamflow values at the corresponding ungauged sites are calculated as below.

$$iQ_{ugHMS}(t) = Q_{ugHMS}(t) + \sum_{i=1}^{G} ie_{gHMS,i}(t), \tag{5}$$

where $i = 1, 2, \ldots\ldots, G$

where, $Q_{gHMS}(t)$ and $Q_{ugHMS}(t)$ are the HEC-HMS computed flows at the gauged and ungauged sites. $Q_o(t)$ is an average observed flow at the gauged site; $ie_{gHMS}(t)$ is the updated flow error(s) from the gauged site(s) for G gauging sites; $iQ_{ugHMS}(t)$ is the updated flow at the ungauged site; and $t = 1$ to N is the time step.

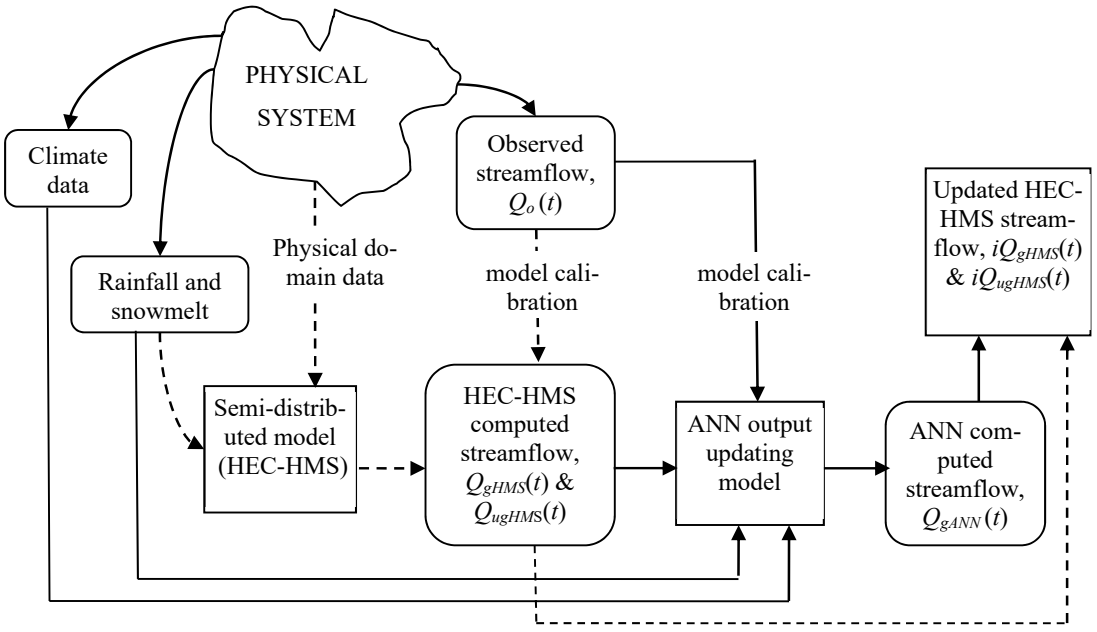

Fig. 1. Schematic diagram of the output updating procedure for gauged and ungauged sites of physically based model.

The hybrid procedure of HEC-HMS and ANN models described above consumes less computation time and provides faster and accurate updates on the HEC-HMS model for both recent and future streamflow hydrographs. The output error of the ungauged site can be improved using the updated error of the corresponding streamflow at the gauged site(s). This way, the information on the updated streamflow hydrographs at the gauged and/or ungauged streamflow sites can be used in water resources and watershed management.

Bayesian regularization neural network with Levenberg-Marquardt algorithm

Bayesian regularization of neural networks can prevent overfitting and underfitting. This approach applies an early learning stopping procedure as soon as the overtraining signal starts to appear. Overtraining signal can be observed when testing the trained neural network with unknown input datasets and predicting output with the highest accuracy. A multilayer feed-forward network associated with the Levenberg-Marquardt (LM) algorithm proves to be faster and more effective in finding optimal results (Anctil et al., 2003; Bertsekas and Tsitsiklis, 1996). According to Hagan and Menhaj (1994), the LM algorithm belongs to the category of second-order nonlinear optimization techniques. The performance of ANN model was superior when the Bayesian regularization was used with LM algorithm in training the multilayer feed-forward network (Anctil et al., 2003; Foresee and Hagan, 1997; Parent et al., 2008).

This study has applied a multilayer feed-forward network with a single hidden sigmoid and linear output layer, LM algorithm and Bayesian regularization. In Bayesian framework, a term that consists of mean of the sum of squares of the network weights and biases, F_w, is automatically added to the typical error function, F_e with their parameters, α and β to improve generalization, as given in the following (MacKay, 1992).

$$F = \beta F_e + \alpha F_w = \beta \sum_{i=1}^{N} e_i^2 + \alpha \sum_{i=1}^{M} W_i \tag{6}$$

where, F is the error function; e, is the network error, the difference between the desired flow, Q_o, and the ANN output, Q_{gANN}, for N number of training inputs; W is the network weights and biases for M total number of weights; α and β are the error function parameters. The algorithm steps for training the ANN model are as follows:

1. Initialize the error function parameters, α and β, and the weights (Nguyen and Widrow, 1990).
2. Present all inputs of size N to the network, and compute the network errors, e. Then, compute the error function, F, over all inputs as in Eq. 6.
3. Take one step of the LM algorithm to minimize the error function.
4. Compute the Hessian matrix, **H**, and the gradient, **g**, using the Jacobian matrix, **J**, that contains the first derivatives of the network errors with respect to the weights and biases, as follows:

$$\mathbf{H} = \frac{\partial^2 F}{\partial w^2} = \mathbf{J}^T \mathbf{J} \tag{7}$$

$$\mathbf{g} = \frac{\partial F}{\partial w} = \sum \frac{\partial e}{\partial w} \mathbf{e} = \mathbf{J}^T \mathbf{e} \tag{8}$$

5. Compute the parameters with new values, $\alpha = \gamma/(2F_w)$ and $\beta = (N-\gamma)/(2F_e)$, using the value of the effective number of parameters $\gamma = N - 2\alpha\ \mathrm{tr}(\mathbf{H})^{-1}$.
6. Solve the ANN weight, using the LM update given in the following:

$$\mathbf{W}_{k+1} = \mathbf{W}_k - \Delta\mathbf{W} = \mathbf{W}_k - [\mathbf{H} + \mu\mathbf{I}]^{-1}\mathbf{g} \tag{9}$$

where, $\Delta\mathbf{W}$ is the updated weight, $\mathbf{W}_k$ is the weight matrix at training iteration (k), $\mathbf{I}$ is the identity matrix, and μ is a scalar that controls the learning process.

7. Recompute the error function of ANN model, F_{k+1}, from Eq. (6) using the new weight $\mathbf{W}_{k+1}$ obtained from step 6. If the new error is reduced ($F_{k+1} < F_k$), then LM algorithm decreases the μ by μ^-, the new weight $\mathbf{W}_{k+1}$ is calculated, and the process starts again from step 2; otherwise, the algorithm increases the μ by μ^+, and the weight of $\Delta\mathbf{W}$ is recalculated from step 6; The default values of $\mu^+ = 10$ and $\mu^- = 0.1$ are usually used.
8. The training procedure is considered to converge when the effective number of parameters, γ has converged, or the error was reduced to some predefined error goal.

Model evaluation criteria

The performance predictions of the ANN updated model and HEC-HMS model for the gauged streamflow locations are evaluated on training, validation and testing datasets. The overall performance of the trained ANN model is evaluated using the correlation coefficient of linear regression, R, in Eq. (10). A high number of $R = 1.0$ means perfect statistical correlation and a low number of $R = 0.0$ means there is no correlation at all. The success measurement of sensitivity analysis for choosing the input variables is based on the root mean square error (*RMSE*) given by Eq. (11), which measures the level of fitness of the ANN model and HEC-HMS model compared with the observed data. This measure ignores the importance of low and high flows (Coulibaly et al., 2001). The peak flow criterion (*PFC*) in Eq. (12), identifies the accuracy of predicting peak flows of ANN and HEC-HMS models for flood flow simulation. The mean absolute error (*MAE*), given by Eq. (13), measures the global goodness of the fit of the forecasted error (the difference between the observed data and the model predicted output). The *MAE* is similar to the *RMSE*, but they differ in their weighting of the errors. Lower values of *RMSE*, *PFC* and *MAE* indicate a good model fit to the observation data. The correlation between the simulated hydrograph and the observed hydrograph is evaluated using the Nash-Sutcliffe coefficient of efficiency (Nash and Sutcliffe, 1970), *EI*, given by Eq. (14), which ranges from negative infinity to 1.0. An *EI* value of 1.0 means a perfect agreement between the observed and simulated hydrographs. The *EI* value equal to or less than 0.0 indicates that the one-parameter "no knowledge" model is better than simulation model output. In this case, the model is not suitable to simulate rainfall-runoff process for the given catchment. Finally, both observed and predicted flow hydrographs for the testing dataset are plotted for visual evaluation of the output for periods of low and high flows.

$$R = \frac{\sum_{t=1}^{N} (Q_t - Q_{ave})(\hat{Q}_t - \hat{Q}_{ave})}{\sqrt{\sum_{t=1}^{N} (Q_t - Q_{ave})^2 (\hat{Q}_t - \hat{Q}_{ave})^2}} \tag{10}$$

$$RMSE = \left[\frac{1}{N} \sum_{t=1}^{N} (Q_t - \hat{Q}_t)^2 \right]^{1/2} \quad (11)$$

$$PFC = \frac{\left(\sum_{t=1}^{NP} (Q_t - \hat{Q}_t)^2 Q_t^2 \right)^{1/4}}{\left(\sum_{t=1}^{NP} Q_t^2 \right)^{1/2}} \quad (12)$$

$$MAE = \frac{1}{N} \sum_{t=1}^{N} \left| Q_t - \hat{Q}_t \right| \quad (13)$$

$$EI = 1 - \frac{\sum_{t=1}^{N} (Q_t - \hat{Q}_t)^2}{\sum_{t=1}^{N} (Q_t - Q_{ave})^2} \quad (14)$$

where $\hat{Q}$ is the ANN updated or HEC-HMS predicted streamflow, Q is the observed streamflow at recent time t, Q_{ave} is the average streamflow, N is the number of observations, and NP is the number of peak flows greater than one-third of the mean peak flow.

STUDY AREA

Description of Upper Thames River watershed

The methodology of output updating is presented for the Upper Thames River watershed located in the southwestern Ontario, Canada. The region comprises four counties, i.e. Perth, Middlesex, Huron and Oxford. There are two main tributaries of the Thames River, namely the North branch (1,750 km^2) and the East branch (1,360 km^2). They converge at forks near the center of the city of London and exits the outlet of watershed near Byron. The watershed receives 1,000 mm of annual precipitation. Estimated annual discharge measured at Byron station is 35.9 m^3·s^{-1}. About 60% of the annual precipitation is lost through evaporation, transpiration, infiltration, etc. The slope at the upper reaches of the Thames basin is close to 1.9 m·km^{-1} and is much flatter at lower reaches with less than 0.2 m·km^{-1} (after Wilcox et al., 1998). The Thames River flows are attenuated by three major reservoirs, Wildwood, Fanshawe and Pittock, which were all built in the mid-1960's for the purpose of flood management. Since then, the utilization of reservoirs expanded also to the low flow maintenance and recreation. The Upper Thames River watershed has historically experienced severe flooding since the 1700s. By the late 1930s and early 1940s, flood events forced the formation of the Conservation Authorities in 1946 to provide solutions for problems associated with flooding. The more recent floods include March 1977, September 1986, July 2000, April 2008, and December 2008 (UTRCA, 2009). Flooding most frequently occurs after the spring snow melts and summer storms (Prodanovic and Simonovic, 2006).

Input data

Several weather stations around the Upper Thames River watershed are used to provide point measurements of daily temperature and precipitation and for estimating the total rainfall and snowmelt. The weather monitoring stations (with identification numbers) listed in Table 1 and the rainfall data from the monitoring stations listed in Table 2 are used to calculate the precipitation (total rainfall and snowmelt) for each sub-watershed of the HEC-HMS model. Other meteorological data from the nearest monitoring sites at Stratford (solar radiation), Wildwood Dam (evaporation) and London (temperature, wind speed, wind direction, station pressure, visibility, and humidity) are used. These historical datasets are obtained from Environment Canada (EC) and the Upper Thames River Conservation Authority (UTRCA). Two gauged streamflow locations, Mitchell and Stratford, are chosen in the output updating of the HEC-HMS model of the Upper Thames River watershed. The updated streamflow values from these gauged sites obtained from the ANN model simulation are then used to update the simulated streamflow values for the ungauged site of JR750 (refer Fig. 2(a)). The Mitchell SG, and Stratford SG of the HEC-HMS model represent the Mitchell and Stratford gauged sites.

Table 1. Location of the weather monitoring stations.

ID Number*	Station	Latitude (deg N)	Longitude (deg W)
6120819	Blyth	43° 43' 00"	81° 23' 00"
6142066	Dorchester	43° 00' 00"	81° 02' 00"
6142295	Embro Innes	43° 15' 00"	80° 56' 00"
6122370	Exeter	43° 21' 00"	81° 30' 00"
6142420	Foldens	43° 01' 00"	80° 47' 00"
6142803	Glen Allan	43° 41' 00"	80° 43' 00"
6144475	London CS	43° 02' 00"	81° 09' 00"
6148105	Stratford MOE	43° 22' 00"	81° 00' 00"
6137362	St. Thomas WPCP	42° 46' 00"	81° 12' 00"
6149387	Waterloo Wellington A	43° 27' 00"	80° 23' 00"
6149625	Woodstock	43° 08' 00"	80° 46' 00"
6129660	Wroxeter	43° 52' 00"	81° 09' 00"
6127514	Sarnia Airport	43° 00' 00"	82° 18' 00"
6147188	Roseville	43° 21' 00"	80° 28' 00"

Table 2. Location of precipitation monitoring stations.

Station	Latitude (deg N)	Longitude (degW)	Station	Latitude (deg N)	Longitude (degW)
Avon	43° 21'	81° 07'	Orr dam	43° 22'	80° 59'
Conestogo	43° 33'	80° 31'	Oxbow Cr.	42° 58'	81° 25'
Dingman Creek.	42° 56'	81° 21'	Parkhill	43° 10'	81° 42'
Dutton	42° 40'	81° 32'	Pittock	43° 16'	80° 49'
Ethel	43° 43'	81° 07'	Plover Mills	43° 09'	81° 11'
Exeter	43° 21'	81° 29'	Reynolds	42° 59'	80° 57'
Ingersoll	43° 03'	80° 53'	Springbank	43° 04'	81° 40'
Innerkip	43° 12'	80° 41'	St. Mary's	43° 15'	81° 11'
Listowel	43° 45'	80° 58'	Stratford	43° 22'	81° 00'
London CS	43° 02'	81° 09'	Thamesford	43° 04'	81° 00'
Medway Creek	43° 00'	81° 17'	Trout Creek	43° 17'	80° 58'
Millbank	43° 35'	80° 44'	Waubuno	43° 00'	81° 07'
Mitchell	43° 27'	81° 12'	Woodstock	43° 08'	80° 46'
New Hamburg	43° 22'	80° 43'	Fanshawe	43° 02' 31"	81° 10'

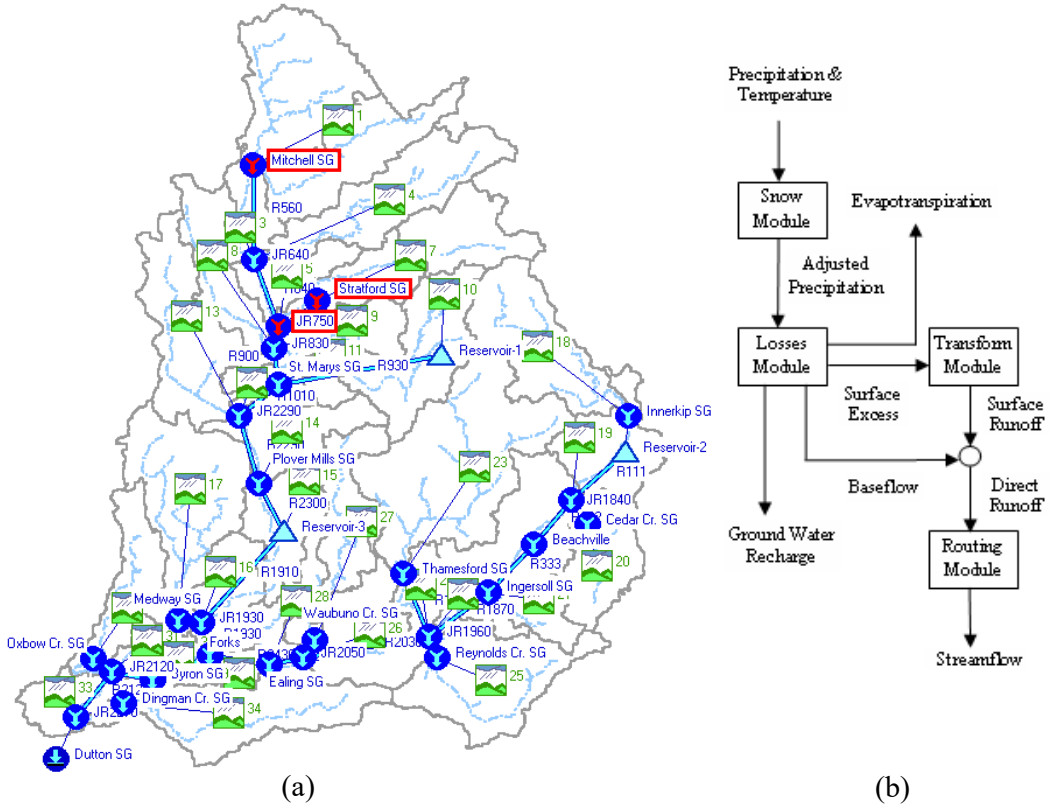

Fig. 2. (a) The HEC-HMS hydrological model of Upper Thames River watershed. (b) The hydrological model structure (Cunderlik and Simonovic, 2004).

HEC-HMS hydrological model

The first hydrological model of the Upper Thames River watershed was developed using the Hydrologic Modeling System (HEC-HMS) version 2.2.2 (USACE, 2000). As shown in Fig. 2(a), the HEC-HMS model consists of thirty-two sub-watersheds, twenty-one river reaches and three reservoirs. The details can be found in Cunderlik and Simonovic (2004). In order to speed up the processing of many hydrological simulations, the computational engine of HEC-HMS model was later re-programmed in the Java programming language. The HEC-HMS model as shown in Fig. 2(b) is separated into several different modules. First, the snow module requires input data of measured precipitation and air temperature for simulating rainfall and snowmelt. Mean areal precipitation of each sub-watershed is computed for interpolation by the Inverse Distance Weighting (IDW) method.

The interpolated sub-watershed precipitation and temperature are used to separate input model precipitation into rainfall and snowfall. Snowmelt computed by a snow accumulation and melt module is added to the liquid precipitation (or rainfall) to produce adjusted precipitation. The rainfall and snowmelt were used as the input data in the calibrated HEC-HMS model for the water losses estimation. The water losses module accounts for the amount of the water movement through various conceptual reservoirs within a watershed, such as canopy, land surface, soils, and groundwater. The outputs from this module include evapotranspiration, surface excess, baseflow, and ground water recharge. The surface excess transformed by the transform module generates surface runoff. This is done by performing a convolution of the unit hydrograph with precipitation excess. The surface runoff combined with the baseflow produces the direct runoff. Finally, the flood routing computation module uses the direct runoff as an input to propagate the flood wave along a stream channel.

Neural network model

In the ANN analysis, other meteorological variables considered as input data besides the streamflow and precipitation (rainfall and snowmelt). They include air humidity, wind speed, wind direction, solar radiation, station pressure, evaporation, visibility, and air temperature. The input dataset for the years 2000 to 2005 is used in the ANN training for both Mitchell and Stratford. The autocorrelation and cross-correlation analyses for all these ANN input data are performed to determine the ANN configuration models, which are highly correlated with the recent observed streamflow (Table 3). The Levenberg-Marquardt algorithm with Bayesian regularization approach is used to identify the best input configuration and its number of hidden nodes, through conducting sensitivity analysis of different input variables.

RESULTS AND DISCUSSION

For Mitchell, the input configuration M20 with additional meteorological data including visibility, humidity, wind speed, solar radiation, station pressure, evaporation, air temperature, and wind direction has the minimum *RMSE* value of 1.95 m^3/s with 14 hidden nodes (Tables 4 and 6). For Stratford, the input configuration M20 gave the minimum *RMSE* value of 0.84 m^3/s with 16 hidden nodes (Tables 5 and 7). The best ANN input configurations for Mitchell and Stratford were:

Mitchell: $Q(t) = f\,(e(t–1), Q(t–1), P(t–1), P(t–2), V(t–1), H(t–1), ...Ws(t–1), Sr(t–1), Sp(t–1), E(t–1)), T(t–1), Wd(t–1))$ (12)

Stratford: $Q(t) = f\,(e(t–1), Q(t–1), P(t–1), P(t–2), Sp(t–1), H(t–1), ...V(t–1), Ws(t–1), Sr(t–1), E(t–1), T(t–1), Wd(t–1))$ (13)

A multilayer feed-forward network with a range of 5 to 20 hidden nodes were successively trained and the optimal performance of test dataset was obtained within a pool of 25 repetitions. This implies that the selected configuration was among the top 14% of the distribution of all possible configurations, with 95% confidence (Iyer and Rhinehart, 1999). Before training, all mean and standard deviation values of the input configurations were constantly normalized.

The performance results of the ANN updated and HEC-HMS models on training, validation and test datasets for Mitchell and Stratford are summarized in Table 8. For all the datasets of Mitchell and Stratford, the Nash-Sutcliffe coefficients (*EI*) performed in Table 8 documented impressive performance of the ANN updated model and a very poor performance of the HEC-HMS model. The ANN updated and HEC-HMS simulated hydrographs are compared against observed streamflow in Figs. 3 and 4, while the updated HEC-HMS streamflow hydrograph for the ungauged site, JR750, is shown in Fig. 5. The HEC-HMS models from Figs 3 and 4 performed poorly during only one event when the simulated streamflow was delayed and overestimated, and a few earlier, smaller events that were not simulated at all. Modelling uncertainty can be related to different input variables used in the HEC-HMS model and in the ANN updated model. In calibration of the HEC-HMS model, Cunderlik

Table 3. The autocorrelation (AC) and cross-correlation (XC) results of Mitchell and Stratford.

					Mitchell					
Lags	AC(*Q*)	XC(*P*)	XC(*Sr*)	XC(*H*)	XC(*Sp*)	XC(*T*)	XC(*V*)	XC(*Wd*)	XC(*Ws*)	XC(*E*)
0	1.0	0.1	–0.2	0.1	–0.2	–0.1	–0.1	0.1	0.2	–0.2
1	0.7	0.4	–0.2	0.2	–0.2	–0.1	–0.2	0.0	0.2	–0.2
2	0.5	0.3	–0.2	0.2	–0.1	–0.1	–0.2	–0.1	0.1	–0.2
3	0.3	0.1	–0.1	0.1	0.0	–0.1	–0.1	–0.1	0.1	–0.2
4	0.2	0.1	–0.1	0.1	0.0	–0.1	–0.1	0.0	0.1	–0.2
					Stratford					
Lags	AC (*Q*)	XC(*P*)	XC(*Sr*)	XC(*H*)	XC(*Sp*)	XC(*T*)	XC(*V*)	XC(*Wd*)	XC(*Ws*)	XC(*E*)
0	1.0	0.2	–0.2	0.2	–0.2	–0.1	–0.1	0.1	0.2	–0.2
1	0.7	0.5	–0.2	0.2	–0.2	–0.1	–0.2	0.0	0.2	–0.2
2	0.4	0.3	–0.1	0.1	–0.1	–0.1	–0.1	–0.1	0.1	–0.2
3	0.3	0.2	–0.1	0.1	0.0	–0.1	–0.1	–0.1	0.1	–0.2
4	0.2	0.1	–0.1	0.1	0.0	–0.1	–0.1	0.0	0.1	–0.2

where, *Q* is daily average streamflow (m^3/s), *P* is total rainfall and snowmelt (mm), *V* is average visibility (km), *H* is relative humidity (%), *Ws* is average wind speed (km/h), *Sr* is maximum solar radiation (MJ m^{-2} day^{-1}), *Sp* is minimum station pressure (kPa), *E* is average evaporation (mm day^{-1}), *T* is average temperature (°C), and *Wd* is average wind direction (10's Deg).

Table 4. The ANN input configuration models for Mitchell.

M1:	e_{t-1}
M2:	e_{t-1} and Q_{t-1}
M3:	e_{t-1} , Q_{t-1} and Q_{t-2}
M4:	e_{t-1} , Q_{t-1} and P_{t-1}
M5:	e_{t-1}, Q_{t-1}, P_{t-1}, and P_{t-2}
M6:	e_{t-1}, Q_{t-1}, P_{t-1}, P_{t-2} and T_{t-1}
M7:	e_{t-1}, Q_{t-1}, P_{t-1}, P_{t-2} and E_{t-1}
M8:	e_{t-1}, Q_{t-1}, P_{t-1}, P_{t-2} and Sr_{t-1}
M9:	e_{t-1}, Q_{t-1}, P_{t-1}, P_{t-2} and Ws_{t-1}
M10:	e_{t-1}, Q_{t-1}, P_{t-1}, P_{t-2} and Sp_{t-1}
M11:	e_{t-1}, Q_{t-1}, P_{t-1}, P_{t-2} and V_{t-1}
M12:	e_{t-1}, Q_{t-1}, P_{t-1}, P_{t-2} and H_{t-1}
M13:	e_{t-1}, Q_{t-1}, P_{t-1}, P_{t-2} and Wd_{t-1}
M14:	e_{t-1}, Q_{t-1}, P_{t-1}, P_{t-2}, V_{t-1} and H_{t-1}
M15:	e_{t-1}, Q_{t-1}, P_{t-1}, P_{t-2}, V_{t-1}, H_{t-1} and Ws_{t-1}
M16:	e_{t-1}, Q_{t-1}, P_{t-1}, P_{t-2}, V_{t-1}, H_{t-1}, Ws_{t-1} and Sr_{t-1}
M17:	e_{t-1}, Q_{t-1}, P_{t-1}, P_{t-2}, V_{t-1}, H_{t-1}, Ws_{t-1}, Sr_{t-1} and Sp_{t-1}
M18:	e_{t-1}, Q_{t-1}, P_{t-1}, P_{t-2}, V_{t-1}, H_{t-1}, Ws_{t-1}, Sr_{t-1}, Sp_{t-1} and E_{t-1}
M19:	e_{t-1}, Q_{t-1}, P_{t-1}, P_{t-2}, V_{t-1}, H_{t-1}, Ws_{t-1}, Sr_{t-1}, Sp_{t-1}, E_{t-1} and T_{t-1}
M20	e_{t-1}, Q_{t-1}, P_{t-1}, P_{t-2}, V_{t-1}, H_{t-1}, Ws_{t-1}, Sr_{t-1}, Sp_{t-1}, E_{t-1}, T_{t-1} and Wd_{t-1}

where, e is the output error of the HEC-HMS model (m^3/s), and t is the recent time and delayed daily three times t–1, t–2 and t–3.

Table 5. The ANN input configuration models for Stratford.

M1:	e_{t-1}
M2:	e_{t-1} and Q_{t-1}
M3:	e_{t-1}, Q_{t-1} and Q_{t-2}
M4:	e_{t-1}, Q_{t-1}, P_{t-1}, P_{t-2} and P_{t-3}
M5:	e_{t-1}, Q_{t-1}, P_{t-1} and P_{t-2}
M6:	e_{t-1}, Q_{t-1}, P_{t-1}, P_{t-2} and T_{t-1}
M7:	e_{t-1}, Q_{t-1}, P_{t-1}, P_{t-2} and E_{t-1}
M8:	e_{t-1}, Q_{t-1}, P_{t-1}, P_{t-2} and Sr_{t-1}
M9:	e_{t-1}, Q_{t-1}, P_{t-1}, P_{t-2} and Ws_{t-1}
M10:	e_{t-1}, Q_{t-1}, P_{t-1}, P_{t-2} and Sp_{t-1}
M11:	e_{t-1}, Q_{t-1}, P_{t-1}, P_{t-2} and V_{t-1}
M12:	e_{t-1}, Q_{t-1}, P_{t-1}, P_{t-2} and H_{t-1}
M13:	e_{t-1}, Q_{t-1}, P_{t-1}, P_{t-2} and Wd_{t-1}
M14:	e_{t-1}, Q_{t-1}, P_{t-1}, P_{t-2}, Sp_{t-1} and H_{t-1}
M15:	e_{t-1}, Q_{t-1}, P_{t-1}, P_{t-2}, Sp_{t-1}, H_{t-1} and V_{t-1}
M16:	e_{t-1}, Q_{t-1}, P_{t-1}, P_{t-2}, Sp_{t-1}, H_{t-1}, V_{t-1} and Ws_{t-1}
M17:	e_{t-1}, Q_{t-1}, P_{t-1}, P_{t-2}, Sp_{t-1}, H_{t-1}, V_{t-1}, Ws_{t-1} and Sr_{t-1}
M18:	e_{t-1}, Q_{t-1}, P_{t-1}, P_{t-2}, Sp_{t-1}, H_{t-1}, V_{t-1} Ws_{t-1}, Sr_{t-1} and E_{t-1}
M19:	e_{t-1}, Q_{t-1}, P_{t-1}, P_{t-2}, Sp_{t-1}, H_{t-1}, V_{t-1}, Ws_{t-1}, Sr_{t-1}, E_{t-1} and T_{t-1}
M20:	e_{t-1}, Q_{t-1}, P_{t-1}, P_{t-2}, Sp_{t-1}, H_{t-1}, V_{t-1}, Ws_{t-1}, Sr_{t-1}, E_{t-1}, T_{t-1} and Wd_{t-1}

and Simonovic (2004) selected inputs of precipitation and temperature from the 9-year long observation (period from November 1979 to October 1988). A semi-annual parametrization approach recommended by Fleming and Neary (2004) was applied, in which different parameter sets for summer and winter seasons were established. Due to the limited availability of meteorological data, the ANN updated model calibration only uses a 4-year record of daily data from 2000 to 2005. Furthermore, the datasets (training, validation, and testing) used in the updated models are selected through implementing data cross-validation, extreme data partition, and trial and error methods. The performance results suggest improvement in the *RMSE* values of the trained networks when additional meteorological data is used.

Table 8 shows that for the training datasets of Mitchell and Stratford, the ANN models have updated with the lowest *RMSE* of 1.930 m^3/s and a perfect agreement updating of observed streamflow values with the highest *EI* of 0.965 and 0.949, respectively. Compared to these ANN updated results, the HEC-HMS model results had a larger absolute error with higher *RMSE* of 9.782 m^3/s and not a good agreement with observed streamflow with low *EI* of 0.097 and –0.150, respectively. For

Table 6. The *RMSE* sensitivity results of the ANN input configuration models for Mitchell.

Unit: [m^3/s]

	Number of hidden nodes															
Models	5	6	7	8	9	10	11	12	13	**14**	15	16	17	18	19	20
M1	4.39	4.38	4.31	4.33	4.43	4.92	4.61	5.15	4.74	4.94	5.15	4.37	5.04	4.33	4.35	4.39
M2	2.70	2.66	2.65	2.68	2.70	2.67	2.72	2.68	2.67	2.63	2.62	2.63	2.55	2.59	2.56	2.53
M3	2.59	2.66	2.59	2.58	2.60	2.60	2.62	2.63	2.59	2.60	2.72	2.63	2.63	2.63	2.65	2.64
M4	2.63	2.71	2.61	2.77	2.57	2.56	2.57	2.55	2.62	2.71	2.57	2.60	2.53	2.58	2.52	2.63
M5	2.41	2.38	2.43	2.38	2.44	2.42	2.37	2.48	2.39	2.45	2.38	2.38	2.39	2.44	2.36	2.38
M6	2.36	2.42	2.40	2.39	2.39	2.34	2.41	2.34	2.44	2.49	2.35	2.39	2.32	2.34	2.33	2.52
M7	2.43	2.36	2.42	2.38	2.37	2.38	2.39	2.36	2.40	2.45	2.43	2.36	2.43	2.46	2.30	2.35
M8	2.39	2.52	2.31	2.34	2.36	2.29	2.28	2.33	2.30	2.32	2.31	2.27	2.30	2.30	2.26	2.27
M9	2.43	2.40	2.41	2.35	2.37	2.62	2.35	2.39	2.43	2.34	2.41	2.37	2.52	2.34	2.42	2.52
M10	2.43	2.54	2.39	2.45	2.39	2.31	2.34	2.41	2.33	2.35	2.32	2.33	2.44	2.36	2.43	2.37
M11	2.16	2.14	2.27	2.18	2.24	2.17	2.18	2.16	2.18	2.08	2.22	2.24	2.17	2.21	2.25	2.18
M12	2.28	2.24	2.26	2.32	2.29	2.27	2.31	2.23	2.38	2.24	2.32	2.37	2.35	2.37	2.38	2.37
M13	2.43	2.44	2.31	2.36	2.40	2.34	2.26	2.30	2.29	2.40	2.32	2.29	2.30	2.30	2.33	2.24
M14	2.25	2.18	2.19	2.17	2.17	2.11	2.07	2.31	2.12	2.26	2.34	2.32	2.24	2.21	2.19	2.38
M15	2.20	2.20	2.27	2.13	2.26	2.31	2.22	2.20	2.13	2.20	2.22	2.18	2.30	2.28	2.33	2.14
M16	2.20	2.08	2.12	2.07	2.11	2.05	2.12	2.13	2.11	2.18	2.07	2.21	2.12	2.12	2.14	2.22
M17	2.14	2.10	2.09	2.02	2.08	2.06	2.00	2.10	2.05	2.19	2.11	2.15	2.12	2.11	2.22	2.14
M18	2.17	2.04	2.12	2.11	2.06	2.07	2.00	2.10	2.04	2.02	2.11	2.13	2.15	2.03	2.14	2.17
M19	2.22	2.12	2.15	2.04	2.10	2.24	2.07	2.17	2.15	2.41	2.15	2.20	2.07	2.15	2.22	2.11
M20	2.15	2.21	2.10	2.15	2.17	2.13	2.20	2.14	2.10	**1.95**	2.17	2.10	1.99	2.15	2.10	2.29

Table 7. The *RMSE* sensitivity results of the ANN input configuration models for Stratford.

Unit: [m^3/s]

	Number of hidden nodes														
Model	6	7	8	9	10	11	12	13	14	15	**16**	17	18	19	20
M1	1.62	1.59	1.59	1.56	1.54	1.56	1.56	1.54	1.59	1.54	1.54	1.53	1.55	1.53	1.55
M2	1.13	1.13	1.11	1.09	1.09	1.09	1.10	1.11	1.09	1.12	1.10	1.10	1.06	1.09	1.04
M3	1.24	1.19	1.23	1.18	1.19	1.18	1.21	1.17	1.24	1.21	1.17	1.21	1.22	1.17	1.19
M4	1.13	1.04	1.06	1.02	0.99	1.03	0.98	1.03	1.00	1.05	1.03	1.05	0.99	0.98	0.99
M5	1.18	1.16	1.23	1.13	1.05	1.16	1.17	1.11	1.10	1.21	1.11	1.17	1.15	1.16	1.08
M6	1.08	0.94	1.11	1.05	0.93	1.03	0.98	1.05	1.01	0.98	0.94	0.95	0.92	0.95	1.07
M7	1.01	1.09	0.95	1.04	1.00	0.96	0.98	1.04	0.97	1.00	0.91	0.98	0.93	0.96	0.95
M8	1.07	1.07	1.12	0.98	1.05	1.10	1.02	0.95	0.99	0.98	0.95	1.02	1.01	1.00	0.95
M9	1.01	1.01	1.17	1.02	0.99	1.02	1.02	0.98	1.00	1.03	0.91	1.04	0.96	0.94	1.09
M10	1.12	1.01	1.11	1.03	1.08	1.03	1.04	1.00	1.04	1.00	1.05	1.01	1.07	1.00	0.96
M11	1.12	1.06	1.07	1.08	1.17	1.04	1.15	1.02	1.03	1.05	0.93	0.97	1.01	1.03	1.04
M12	1.07	1.01	1.04	1.10	0.98	1.02	0.95	0.96	0.99	0.94	0.98	1.02	0.98	0.99	0.93
M13	1.08	1.17	1.10	1.08	1.03	1.12	1.09	1.00	1.05	0.97	1.07	1.05	1.02	1.09	1.00
M14	1.16	1.07	1.04	1.07	1.07	0.91	1.01	0.93	0.97	0.92	0.97	0.91	0.94	0.97	0.93
M15	1.06	1.15	1.04	1.11	1.06	1.10	1.12	1.03	0.96	0.99	1.03	1.09	0.93	0.94	0.92
M16	1.13	1.06	1.04	1.00	1.04	1.00	1.01	0.96	0.95	0.96	1.02	0.97	1.01	1.00	0.95
M17	1.11	1.04	0.99	1.07	1.07	0.96	1.02	1.02	0.90	1.04	0.94	1.00	0.94	0.90	0.96
M18	1.08	1.04	1.00	0.94	0.94	1.04	1.00	1.04	1.04	0.94	0.98	0.98	0.90	1.00	0.93
M19	1.05	0.96	1.00	1.04	0.98	1.01	0.95	0.93	0.85	0.87	0.95	0.91	0.87	0.97	0.87
M20	1.02	1.01	0.98	0.98	0.93	1.06	0.95	0.85	0.92	0.90	**0.84**	0.96	0.86	0.89	0.86

the validation and test datasets of Mitchell, the ANN models present a slightly higher *EI* of 0.896 and 0.881, while the HEC-HMS models have given a low value of *EI* = 0.072 and negative value of 0.341, respectively. The updated streamflow hydrograph shown in Fig. 3 obtained by the ANN model best matched the observed streamflow hydrograph for the Mitchell test dataset. For the Stratford validation dataset, the ANN model gives an optimal updating of streamflow values with a performance of *EI* = 0.933, while the HEC-HMS model presents an unsatisfactory model performance of *EI* = –0.075. The perfect agreement of *EI* = 0.962 is observed between the ANN updated hydrograph and the observed streamflow hydrograph on Stratford test dataset shown in Fig. 4.

Several other approaches are available for streamflow updating. The methods of Box and Jenkins (1970) such as AR (autoregressive) and ARMA (auto-regressive moving average), and ARMAX (autoregressive moving average with exogenous inputs) are the statistical approaches that are mostly short-time dependent. They do not attempt to represent the hydrological processes that are non-linear in both time and space (Hsu et al., 1995). A fuzzy logic method (Takagi and Sugeno, 1985) is introduced by Xiong and O'Connor (2002) to account the streamflow simulation errors. The membership functions, the fuzzy inference rules, the associated threshold values and the model output are identified, based on subjective decisions made by humans from experience and observation. The subjectivity can be reduced by selecting the suitable membership functions and associated parameters as the model objective through improving the performance of the forecast updating efficiency. The Kalman Filter algorithm is used to upgrade the hydrological model for streamflow prediction by a linear systems analysis (Schreider et al., 2001). The optimality of Kalman filtering relies on the statistical errors with a normal (Gaussian) distribution. In this study, ANN technique is used to update the HEC-HMS hydrological model for solving nonlinear rainfall-runoff processes. ANNs have the capability of learning the relationship between input-output datasets of a complex non-linear system, without prior knowledge of the underlying physical phenomena.

Table 8. Performance results of the ANN and HEC-HMS models.

Station name	Dataset and period	Streamflow (m^3/s)	Simulated model	*RMSE* (m^3/s)	*MAE* (m^3/s)	*EI*	*PFC*	*R*
Mitchell	Training	4.519	HMS	9.782	3.795	0.097	0.395	0.472
	(2002 to 2005)		ANN	1.930	0.992	0.965	0.156	0.982
	Validation	5.277	HMS	10.628	4.018	0.072	0.593	0.396
	(2000)		ANN	3.565	1.562	0.896	0.276	0.947
	Test	4.971	HMS	11.926	4.495	–0.341	0.569	0.456
	(2001)		ANN	3.551	1.503	0.881	0.334	0.939
Stratford	Training	1.945	HMS	3.950	1.501	–0.150	0.449	0.444
	(2000; 2003 to 2005)		ANN	0.833	0.423	0.949	0.151	0.974
	Validation	1.871	HMS	3.653	1.417	–0.075	0.726	0.295
	(2002)		ANN	0.910	0.465	0.933	0.182	0.968
	Test	2.139	HMS	3.718	1.415	0.182	0.664	0.562
	(2001)		ANN	0.804	0.431	0.962	0.208	0.981

where, HMS denotes the HEC-HMS model, and ANN represents the artificial neural network model.

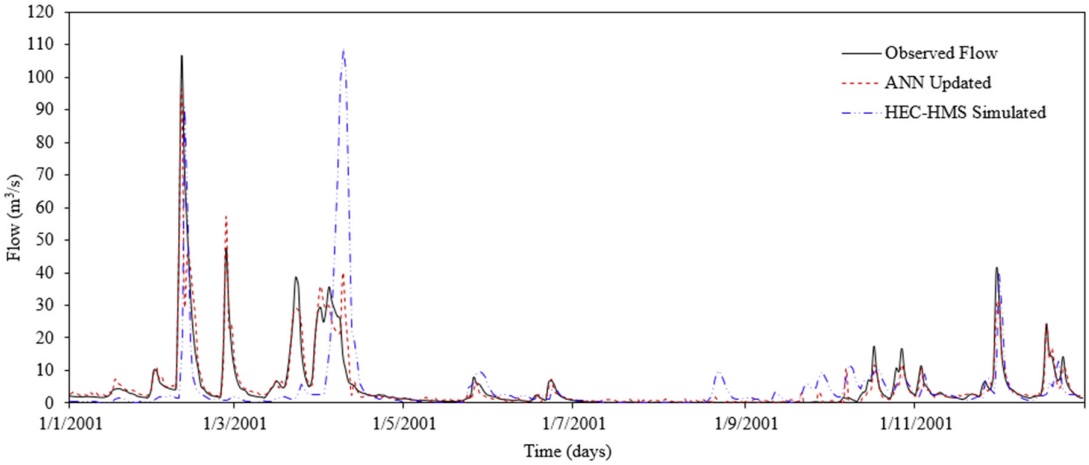

Fig. 3. Comparison of the ANN updated, HEC-HMS simulated and observed flow hydrographs year 2001 for Mitchell.

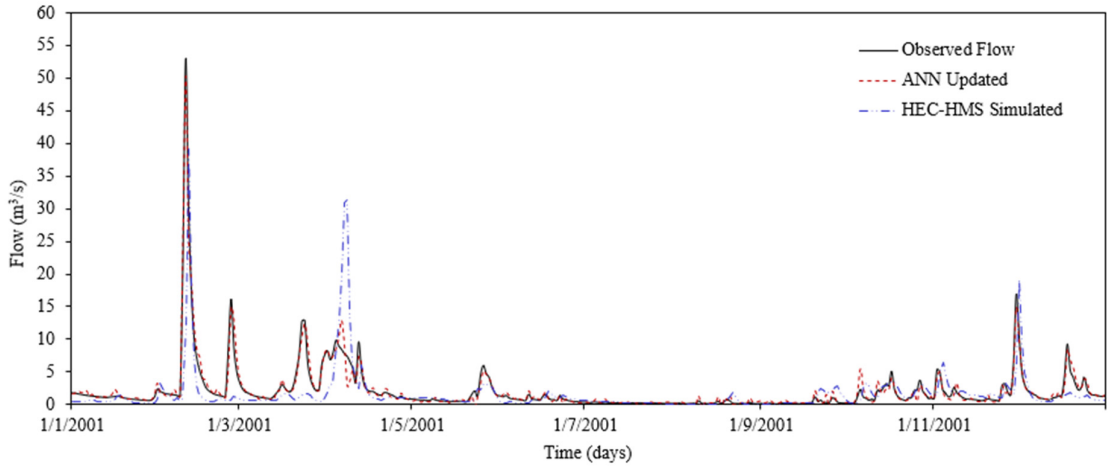

Fig. 4. Comparison of the ANN updated, HEC-HMS simulated and observed flow hydrographs year 2001 for Stratford.

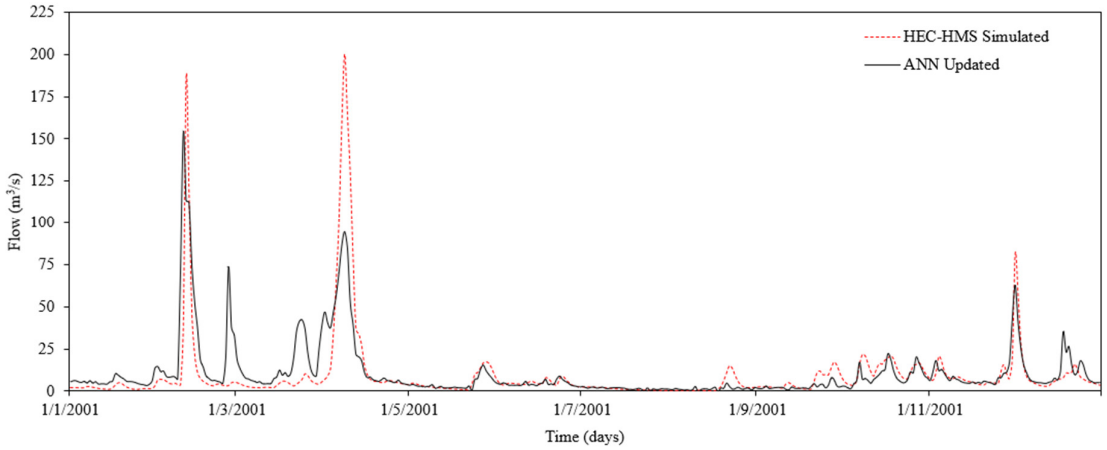

Fig. 5. Comparison of the ANN updated and HEC-HMS simulated hydrographs year 2001 for the ungauged site, JR750.

The valuable information on a large variety of hydrometeorological parameters resulted in a wide range of flow hydrographs could be developed using ANNs.

The limitation of this study is the lack of historical observation data for the neural network training. The ANN models of Mitchell and Stratford are learnt through some observations. This means they are only capable of interpreting data on which they trained. The validation and test periods are also very short (just one year each) to know the real capability of the ANN models in updating streamflow values when tested with a new dataset. Therefore, for the more accurate streamflow updates, these neural networks shall be trained with a larger amount of hydrometeorological observations to learn and model non-linear and complex relationships in the datasets. The ANN model can also perform very well in making predictions on a new dataset and fits so well to it.

The ANN models in this study have been trained and developed based on the hydrometeorological conditions around nearby Mitchell and Stratford locations. Therefore, they cannot be applied and extrapolated to similar or different catchments in other locations with similar patterns of land use and climate. For different catchments, different types of neural network training and modelling using their nearby hydrometeorological conditions are required.

CONCLUSION

This study presents an updating procedure of the HEC-HMS hydrological model based on the neural network approach. The overall results of performance measures (such as *RMSE*, *MAE*, *EI*, *PFC* and *R*) on training, validation and test datasets for Mitchell and Stratford show that the ANN models can lead to more accurate streamflow predictions than the calibrated HEC-HMS model. For all the datasets of Mitchell and Stratford, the ANN models provided the most accurate streamflow values with a satisfactory model of *EI* higher than 0.881. The HEC-HMS models have shown the lowest negative *EI* of –0.314 which means the model was not suitable for streamflow simulations in this study watershed. The use of additional available meteorological data in the ANN model has considerably updated the trained network and resulted in a lower *RMSE* value. The results showed that the use of Bayesian regularization as an objective function in the Levenberg-Marquardt ANN model can reduce the output errors of physically based models.

Acknowledgement. The authors thank the Ministry of Higher Education Malaysia, Universiti Teknologi Malaysia, Collaborative Research Grant, no. vote Q.J130000.2451.09G52 and University of Western Ontario, Canada for their supports of the presented research.

REFERENCES

Abbott, M.B., Bathurst, J.C., Cunge, J.A., O'Connell, P.E., Rasmussen, J., 1986. An introduction to the European Hydrological System – Systeme Hydrologique Europeen (SHE). Part 1. History and philosophy of a physically-based distributed modelling system. Journal of Hydrology, 87, 45–59.

Abebe, A.J., Price, R.K., 2004. Information theory and neural networks for managing uncertainty in flood routing. Journal of Computing in Civil Engineering, 18, 4, 373–380.

Abrahart, R.J., See, L.M., 2007. Neural network modelling of non-linear hydrological relationships. Journal of Earth System Science, 11, 5, 1563–1579.

Ahmad, S., Simonovic, S.P., 2005. An artificial neural network model for generating hydrograph from hydro-meteorological parameters. Journal of Hydrology, 315, 1–4, 236–251.

Anctil, F., Perrin, C., Andreassian, V., 2003. ANN output updating of lumped physically rainfall/runoff forecasting models. Water Resources Bulletin, 39, 5, 1269–1279.

Anctil, F., Claude, M., Charles, P., Vazken, A., 2004. A soil moisture index as an auxiliary ANN input for stream flow forecasting. Journal of Hydrology, 286, 155–167.

Anctil, F., Rat, A., 2005. Evaluation of neural network streamflow forecasting on 47 watersheds. Journal of Hydrology, 10, 1, 85–88.

Asquith, W.H., Slade, R.M., 1997. Regional equations for estimation of peak-stream frequency for natural basins in Texas. Water-Resources Investigations Report 96-4307, U.S. Geological Survey, Austin, Texas.

ASCE Task Committee on Artificial Neural Networks in Hydrology, 2000. Artificial neural networks in hydrology. Journal of Hydrological Engineering, 5, 2, 124–137.

Aytek, A., Asce, M., Alp, M., 2008. An application of artificial intelligence for rainfall-runoff modeling. Journal of Earth System Science, 117, 2, 145–155.

Bertsekas, D.P., Tsitsiklis, J.N., 1996. Neuro-Dynamic Programming. Athena Scientific, Belmont, Massachusetts, USA.

Beven, K.J., 2001. Rainfall-Runoff Modelling: The Primer. John Wiley and Sons, Chichester, UK.

Bhattacharya, B., Solomatine, D.P., 2000. Application of neural networks in stage-discharge relationships. In: Proc. 4th International Conference on Hydroinformatics, Iowa City, USA.

Box, G.E.P., Jenkins, G.M., 1970. Time Series Analysis, Forecasting and Control. Holden-Day, San Francisco, California, 537 p.

Coulibaly, P., Anctil, F., Bobe'e, B., 2001. Multivariate reservoir inflow forecasting using temporal neural networks. Journal of Hydrologic Engineering, 6, 5, 367–376.

Cunderlik, J.M., 2003. Hydrologic Model Selection for the CFCAS Project: Assessment of Water Resources Risk and Vulnerability to Changing Climatic Condition, Water Resources Research Report no. 046. Department of Civil and Environmental Engineering, The University of Western Ontario, London, Ontario, Canada, 38 p. ISBN: (print) 978-0-7714-2622-3; (online) 978-0-7714-2623-0.

Cunderlik, J.M., Simonovic, S.P., 2004. Assessment of water resources risk and vulnerability to changing climatic conditions: Calibration and verification data for the HEC-HMS hydrologic model, Report No. II. Department of Civil and Environmental Engineering, The University of Western Ontario, London, Ontario, Canada.

Devulapalli, R.S., 1995. Flood volume-duration-frequencies for ungaged rural catchment. Ph.D. Dissertation, Civil Engineering, Texas A&M University, College Station, Texas.

Fleming, M., Neary, V., 2004. Continuous hydrologic modeling study with the Hydrologic Modeling System. Journal of Hydrologic Engineering, 9/3, 175–183.

Foresee, F.D., Hagan, M.T., 1997. Gauss-Newton approximation to Bayesian regularization. In: Proc. International Joint Conference on Neural Networks, pp. 1930–1935.

Gan, K.C., McMahon, T.A., O'Neill, I.C., 1991. Transposition of monthly streamflow data to ungauged catchments. Nordic Hydrology, 22, 2, 109–122.

Gosain, A.K., Mani, A., Dwivedi, C., 2009. Hydrological modelling literature review: Report No.1. Indo-Norwegian Institutional Cooperation Program 2009–2011.

Goswami, M., O'Connor, K.M., Bhattarai, K.P., Shamseldin, A.Y., 2005. Assessing the performance of eight real-time updating models and procedures for the Brosna River. Journal of Earth System Science, 9, 4, 394–411.

Govindaraju, R.S., Rao, A.R., 2000. Artificial Neural Networks in Hydrology. Kluwer Academic Publisher, Dordrecht, The Netherlands.

Hagan, M.T., Menhaj, M.B., 1994. Training feedforward networks with Marquardt algorithm. IEEE Transactions on Neural Networks, 5, 6, 989–993.

Hsu, K., Gupta, V.H., Sorroshian, S., 1995. Artificial neural network modeling of the rainfall-runoff process. Water Resources Research, 31, 10, 2517–2530.

Iyer, M.S., Rhinehart, R.R., 1999. A method to determine the required number of neural-network training repetitions. IEEE Transactions on Neural Networks, 10, 2, 427–432.

Jain, A., Srinivasulu, S., 2006. Integrated approach to model decomposed flow hydrograph using artificial neural network and physically techniques. Journal of Hydrology, 317, 3–4, 291–306.

Jennings, M.E., Thomas W.O., Riggs, H.C., 1994. Nationwide Summary of U. S. Geological Survey Regression Equations for Estimating Magnitude and Frequency of Floods for Ungaged Sites. Water-Resources Investigations Report 94-4002, U.S. Geological Survey, Reston, Virginia.

MacKay, D.J.C., 1992. Bayesian interpolation. Neural computation, 4, 3, 415–447.

Moradkhani, H., Hsu, K.L, Gupta, H., Sorooshian, S., 2004. Improved streamflow forecasting using self-organizing radial basis function artificial neural networks. Journal of Hydrology, 295, 1–4, 246–262.

Nash, J.E., Sutcliffe, J.V., 1970. River flow forecasting through conceptual models, Part I - A discussion of principles. Journal of Hydrology, 10, 3, 282–290.

Nguyen, D., Widrow, B., 1990. Improving the learning speed of 2-layer neural networks by choosing initial values of the adaptive weights. In: Proc. International Joint Conference on Neural Networks, 3, 21–26.

Parent, A., Anctil, F., Cantin, V., Boucher, M., 2008. Neural network input selection for hydrological forecasting affected by snowmelt. Water Resources Bulletin, 44, 3, 679–688.

Poff, N.L., Tokar, S., Johnson, P., 1996. Stream hydrological and ecological responses to climate change assessed with an artificial neural network. Limnology and Oceanography, 41, 5, 857–863.

Prodanovic, P., Simonovic, S.P., 2006. Assessment of risk and vulnerability to changing climatic conditions: Inverse Flood Risk Modelling of the Upper Thames River Basin, Report No. VIII. Department of Civil and Environmental Engineering, The University of Western Ontario, London, Ontario, Canada.

Rajurkar, M.P., Kothyari, U.C., Chaube, U.C., 2004. Modeling of the daily rainfall runoff relationship with artificial neural network. Journal of Hydrology, 285, 96–113.

Refsgaard, J.C., 1996. Terminology, modelling protocol and classification of hydrologic model codes. In: Abbott. M.B., Refsgaard, J.C. (Eds.): Distributed Hydrologic Modelling, pp. 41–54.

Schreider, S., Young, P., Jakeman, A., 2001. An application of the Kalman filtering technique for streamflow forecasting in the Upper Murray Basin. Mathematical and Computer Modelling, 33, 733–743.

Takagi, T., Sugeno, M., 1985. Fuzzy identification of systems and its application to modelling and control. IEEE Trans. Systems, Man, and Cybernectics, 15, 116–132.

Thirumalaiah, K., Deo, M.C., 1998. River stage forecasting using artificial neural networks. Journal of Hydrologic Engineering, 3, 1, 26–32.

USACE, 2000. Hydrologic Modelling System HEC–HMS: Technical reference manual. United States Army Corps of Engineers, Hydrologic Engineering Center, Davis, California.

UTRCA, 2009. Inspiring a Healthy Environment: Flooding on the Thames River. Upper Thames River Conservation Authority, London, Ontario, Canada. Available online at http://www.thamesriver.on.ca/Water_Management/flood_history.htm - last accessed January 29, 2010.

Vrugt, J.A., Diks, C.G.H., Gupta, H.V., Bouten, W., Verstraten, J.M., 2005. Improved treatment of uncertainty in hydrologic modeling: combining the strengths of global optimization and data assimilation. Water Resour. Res., 41, 1.

Wardah, T., Abu Bakar, S.H., Bardossy, A., Maznorizan, M., 2008. Use of geostationary meteorological satellite images in convective rain estimation for flash-flood forecasting. Journal of Hydrology, 356, 3–4, 283–298.

Wilcox, I., Quinlan, C., Rogers, C., Troughton, M., McCallum, I., Quenneville, A., Heagy, E., Dool, D., 1998. The Thames River Basin: A Background Study for Nomination under the Canadian Heritage Rivers System. Upper Thames River Conservation Authority, London, Ontario, Canada.

Wurbs, R.A., Sisson, E.D., 1999. Comparative evaluation of methods for distributing naturalized streamflows from gauged to ungauged sites. Technical Report No. 179, College Station: Texas A & M University, Water Resources Institute.

Xiong, L., O'Connor, K.M., 2002. Comparison of four updating models for real-time river flow forecasting. Hydrological Sciences Journal, 47, 4, 621–639.

Xiong, L., O'Connor, K.M., Guo, S., 2004. Comparison of three updating schemes using artificial neural network in flow forecasting. Journal of Earth System Science, 8, 2, 247–255.

Yu, F.X.Y., Pardue, J., Adrian, D.D., 1997. Evaluation of nine models for ungauged urban basins in Louisiana. Journal of the American Water Resources Association, 33, 1, 97–110.

Received 2 June 2022
Accepted 24 April 2023